# Functional polyesters enable selective siRNA delivery to lung cancer over matched normal cells

Yunfeng Yan[a,b], Li Liu[c], Hu Xiong[a,b], Jason B. Miller[a,b], Kejin Zhou[a,b], Petra Kos[a,b], Kenneth E. Huffman[d], Sussana Elkassih[a,b], John W. Norman[a,b], Ryan Carstens[d], James Kim[d,e], John D. Minna[d], and Daniel J. Siegwart[a,b,1]

[a]Simmons Comprehensive Cancer Center, The University of Texas Southwestern Medical Center, Dallas, TX 75390; [b]Department of Biochemistry, The University of Texas Southwestern Medical Center, Dallas, TX 75390; [c]Department of Radiology, The University of Texas Southwestern Medical Center, Dallas, TX 75390; [d]Hamon Center for Therapeutic Oncology Research, The University of Texas Southwestern Medical Center, Dallas, TX 75390; and [e]Department of Internal Medicine, The University of Texas Southwestern Medical Center, Dallas, TX 75390

Edited by Kristi S. Anseth, Howard Hughes Medical Institute, University of Colorado Boulder, Boulder, CO, and approved July 26, 2016 (received for review April 29, 2016)

**Conventional chemotherapeutics nonselectively kill all rapidly dividing cells, which produces numerous side effects. To address this challenge, we report the discovery of functional polyesters that are capable of delivering siRNA drugs selectively to lung cancer cells and not to normal lung cells. Selective polyplex nanoparticles (NPs) were identified by high-throughput library screening on a unique pair of matched cancer/normal cell lines obtained from a single patient. Selective NPs promoted rapid endocytosis into HCC4017 cancer cells, but were arrested at the membrane of HBEC30-KT normal cells during the initial transfection period. When injected into tumor xenografts in mice, cancer-selective NPs were retained in tumors for over 1 wk, whereas nonselective NPs were cleared within hours. This translated to improved siRNA-mediated cancer cell apoptosis and significant suppression of tumor growth. Selective NPs were also able to mediate gene silencing in xenograft and orthotopic tumors via i.v. injection or aerosol inhalation, respectively. Importantly, this work highlights that different cells respond differentially to the same drug carrier, an important factor that should be considered in the design and evaluation of all NP carriers. Because no targeting ligands are required, these functional polyester NPs provide an exciting alternative approach for selective drug delivery to tumor cells that may improve efficacy and reduce adverse side effects of cancer therapies.**

functional polyesters | siRNA | cancer | drug delivery | nanoparticles

Lung cancer is the leading cause of new cancer cases and cancer-related mortality worldwide (1). Most anticancer drugs indiscriminately kill all dividing cells, manifesting in hair loss, fatigue, infection, and other problems (2–4). Extensive efforts have been made to design new drugs that selectively target precise pathways driving the development of specific cancers, but many attractive cancer targets remain undruggable (5, 6). Short interfering RNA (siRNA)-based therapies are a promising alternative approach because they can theoretically silence expression of any oncogene (5, 7, 8). However, siRNA sequences must be carefully designed to minimize off-target effects and toxicity, especially toward healthy cells (9, 10). Improving selectivity to cancer cells would have a transformative impact on the future of both chemotherapeutic small molecule drugs and RNA-based cancer treatment (3, 4, 11, 12). A critical unmet challenge therefore is to design delivery carriers that are specific to cancer cells to improve efficacy and reduce off-target effects to normal cells (4, 10).

Targeted drug delivery traditionally involves modifying the surface of nanoparticles with tumor-specific targeting motifs such as antibodies (13), aptamers (14), transferrin protein (15), short peptides (16), or ligands (17). However, the specific interaction between these motifs and their targets can be reduced in vivo due to conformational change of proteins (18), variable expression of targets on cell surfaces (12), and the masking of ligand display by adsorption of serum proteins on the delivery vehicle (19). As an alternative strategy, we hypothesized that the physicochemical properties of the polymeric carriers alone may enable selective delivery of polymer-siRNA polyplex nanoparticles (NPs) to cancer cells but not normal cells. We show that the physiochemical properties of materials alone can endow selective delivery to specific cells, suggesting a new way to avoid drug side effects, and illuminating the unappreciated reality that NP carriers exhibit cell type-dependent delivery.

A large number of materials have been developed that can effectively deliver nucleic acids, but these systems have not been shown to provide selectivity between cell types (8). We focused on polyesters because they have been safely used in numerous Food and Drug Administration-approved products (20). Nevertheless, scalable synthesis and modification of functional polyesters is an ongoing challenge (21–24). We recently developed a scalable method to yield functional polyesters based on the polycondensation of trimethylolpropane allyl ether and diacyl chlorides with tunable molecular weight (MW) (22). This methodology allows for construction of chemically diverse polyesters because thiol-ene click reactions (25) permit the facile modification of chemical functionality and physical properties. Herein, we have applied this synthetic method to design a polymer library containing 840 functional polyesters with varying MW and chemical identities to maximize potential variance in physicochemical properties to meet siRNA delivery requirements and provide enough structural diversity to discover cancer cell-specific NPs.

To identify cancer cell-specific NPs, we used a matched tumor/normal lung cell line pair (HCC4017/HBEC30-KT), derived

## Significance

**Ideal cancer therapeutics accurately hit tumors and avoid side effects on healthy cells. We used a patient-derived pair of matched cancer/normal cell lines to discover selective nanoparticles that could deliver a cytotoxic siRNA to kill cancer cells and not normal cells. The finding that cells respond differently to the same nanoparticle has profound implications for gene therapy because cell-type specificity of drug carriers in vivo could alter clinical patient outcomes. Our data suggest that selectivity is an underappreciated reality that should be carefully considered when evaluating drug carriers. The combination of both well-defined molecular targets and nanoparticle delivery to targeted cells is likely required to improve cancer drug accuracy in the clinic.**

Author contributions: Y.Y. and D.J.S. designed research; Y.Y., L.L., H.X., J.B.M., K.Z., P.K., K.E.H., S.E., J.W.N., and D.J.S. performed research; Y.Y., L.L., K.E.H., R.C., J.K., and J.D.M. contributed new reagents/analytic tools; Y.Y., L.L., H.X., J.B.M., K.Z., P.K., J.D.M., and D.J.S. analyzed data; D.J.S. directed research; and Y.Y. and D.J.S. wrote the paper.

The authors declare no conflict of interest.

This article is a PNAS Direct Submission.

[1]To whom correspondence should be addressed. Email: daniel.siegwart@utsouthwestern.edu.

This article contains supporting information online at www.pnas.org/lookup/suppl/doi:10.1073/pnas.1606886113/-/DCSupplemental.

from a single female lung cancer patient (26). We report the discovery of selective polyester siRNA polyplex NPs that provide cancer specific therapy (Fig. 1*A*) in vitro and in vivo. We delivered siRNA targeting ubiquitin B (siUBB) (27, 28), which causes cell death in all cell types to evaluate the delivery selectivity to HCC4017 tumor cells over HBEC30-KT normal cells. NPs were identified that showed selective cellular uptake to cancer cells over normal cells followed by reduced transport to lysosomes. Cancer cell growth was also selectively suppressed in colony formation assays. In mice, selective NPs exhibited extended retention in tumor tissues and consequently increased siUBB-mediated apoptosis. Selectivity directly translated to suppression of tumor growth as a therapeutic outcome. The translational potential of selective NPs was further validated by siRNA-mediated knockdown in xenograft and orthotopic lung tumors. Because the selectivity of the delivery vehicles relies only on their physicochemical properties, this eliminated the need to attach additional cell-specific targeting motifs. Therefore, these results provide a unique strategy to suppress the side effects of small RNAs to healthy cells/tissues and improve therapeutic efficacy.

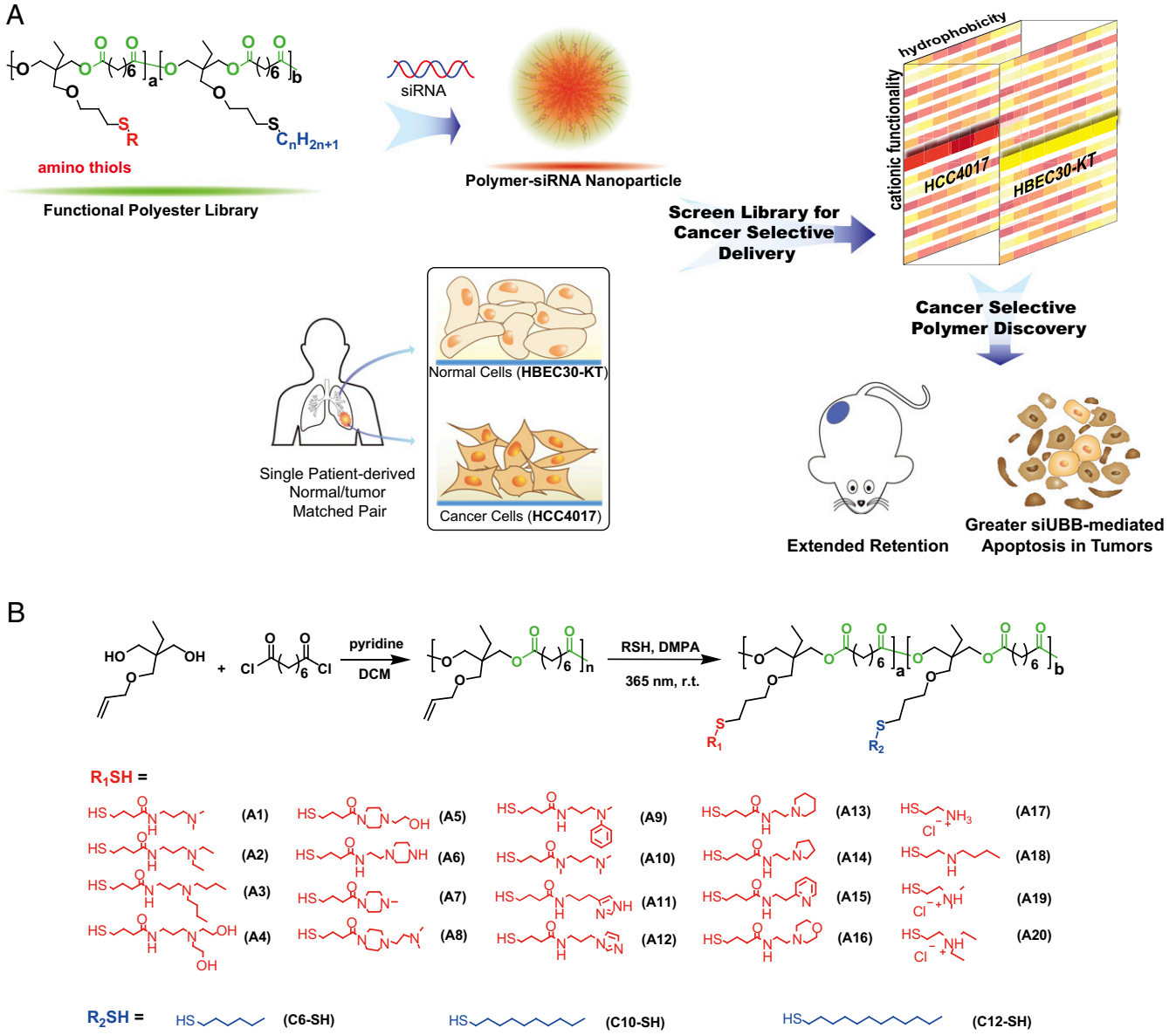


**Fig. 1.** A combinatorial library of functional polyester NPs was screened in a patient-derived normal/tumor cell line pair to discover cancer-selective siRNA delivery materials. (*A*) Degradable polyesters bearing amino and hydrophobic side chains were formulated into siRNA polyplex NPs with variable physiochemical properties. Cancer-selective NPs were identified by using a matched tumor/normal cell line pair (HCC4017/HBEC30-KT) derived from the normal and cancerous lung tissues of a single patient. (*B*) A library of 840 functional polyesters was chemically synthesized for the screening of siRNA delivery to normal/tumor cell lines. Ene-bearing polyesters with varying molecular weight were synthesized by polycondensation of trimethylolpropane allyl ether and suberoyl chloride at room temperature. Polyesters were modified with amino thiols ($R_1SH$) and alkyl thiols ($R_2SH$) to generate a functional polymer library with rich diversity in physicochemical properties [i.e., diverse binding (amine) and NP stabilizing hydrophobic (alkyl) groups, tunable amino/alkyl ratios, and variable length of polymer chains]. Amino thiols are named A followed by a number; alkyl thiols are named C followed by the number of carbons. Functional polyesters with $M_w$ 4,200 g/mol (PE4K) and 8,300 g/mol (PE8K) were modified with all amino thiols (A1–A20) and alkyl thiols (C6–C12) at C:A molar feed ratios of 1:4, 1:2, 1:1, and 2:1. Functionalized polymers are named by the polyester MW, amino modification, and the mole fraction of alkyl modification.

## Results

**A Scalable Method Enabled Synthesis of Polyesters with Diverse Physiochemical Properties to Facilitate Efficacious siRNA Delivery to Cancer Cells.** To evaluate the hypothesis that functional polyplexes might enable selective siRNA delivery, a large library of biocompatible polymers with tunable functionality was required. In this paper, we built upon a scalable synthetic strategy (22) to prepare a combinatorial library of functional polyesters for selective siRNA delivery. To diversify the physicochemical properties of the polyesters, 16 amino thiols were synthesized via aminolysis of γ-thiobutyrolactone (*SI Appendix*, Scheme S1 and Fig. S1). These chemically synthesized amino thiols provided a unique expansion in chemical diversity. Three ene-containing polyesters [weight-average molecular weight ($M_w$) = 4,200, 8,300, and 16,800 g/mol] (*SI Appendix*, Fig. S2) were modified with amino and alkyl thiols with varying ratios via thiol-ene reaction under UV irradiation (Fig. 1*B*) (25). Particular focus was laid on chemical functionalities, including cationic and hydrophobic chains that have been implicated in effective nucleic acid carriers (8, 29–39).

Polymeric carriers must overcome a series of extracellular and intracellular barriers to enable siRNAs to be active inside of tumor cells (7). To verify that this class of functional polyesters can deliver siRNA in vitro, a preliminary 360-member polyester library was first screened in HeLa cells that stably expressed luciferase (HeLa-Luc) (*SI Appendix*, Figs. S3–S5). Initially, the polyesters were modified by only the amino thiols to examine the effect of cationic groups and confirm that this class of materials is capable of silencing luciferase while maintaining low toxicity. Polyesters modified with A3, A5, and A13 were particularly effective, where the silencing depended on the modification degree (*SI Appendix*, Fig. S3). Furthermore, lower MW polyesters ($M_w$ = 4,200 or 8,300) were more effective than higher MW polymers ($M_w$ =16,800). This is consistent with previous reports that examined the effect of poly (β-amino ester) MW on delivery, suggesting that higher MW is optimal for plasmid DNA delivery, whereas lower MW is optimal for the shorter, more rigid siRNA (40–43).

Focusing on the polyesters with lower MWs, we next examined the effect of hydrophobic side chains to enhance the stability of polyplex NPs (33) (*SI Appendix*, Fig. S5). A second functional polyester library of 520 comodified polyesters was synthesized. Polymers are named by the starting MW, followed by the amino thiol and the alkyl thiol feed ratio (e.g., PE4K-A1-0.2C6). Structure-activity analysis of a heat map showing luciferase silencing indicated that the area with lower MW (PE4K) and longer alkyl thiols (C12SH) and the area with higher MW (PE8K) and shorter alkyl thiols (C6SH and C10SH) were the most active. This suggests that, in addition to optimal cationic nature and $pK_a$, effective siRNA delivery requires a balance between the polymer MW and hydrophobicity that relates to physical chain entanglement and intermolecular forces (23, 35, 39, 44). The top-performing polymers show superior delivery activity over the commercial benchmark RNAiMax according to dose–response curves (*SI Appendix*, Fig. S4).

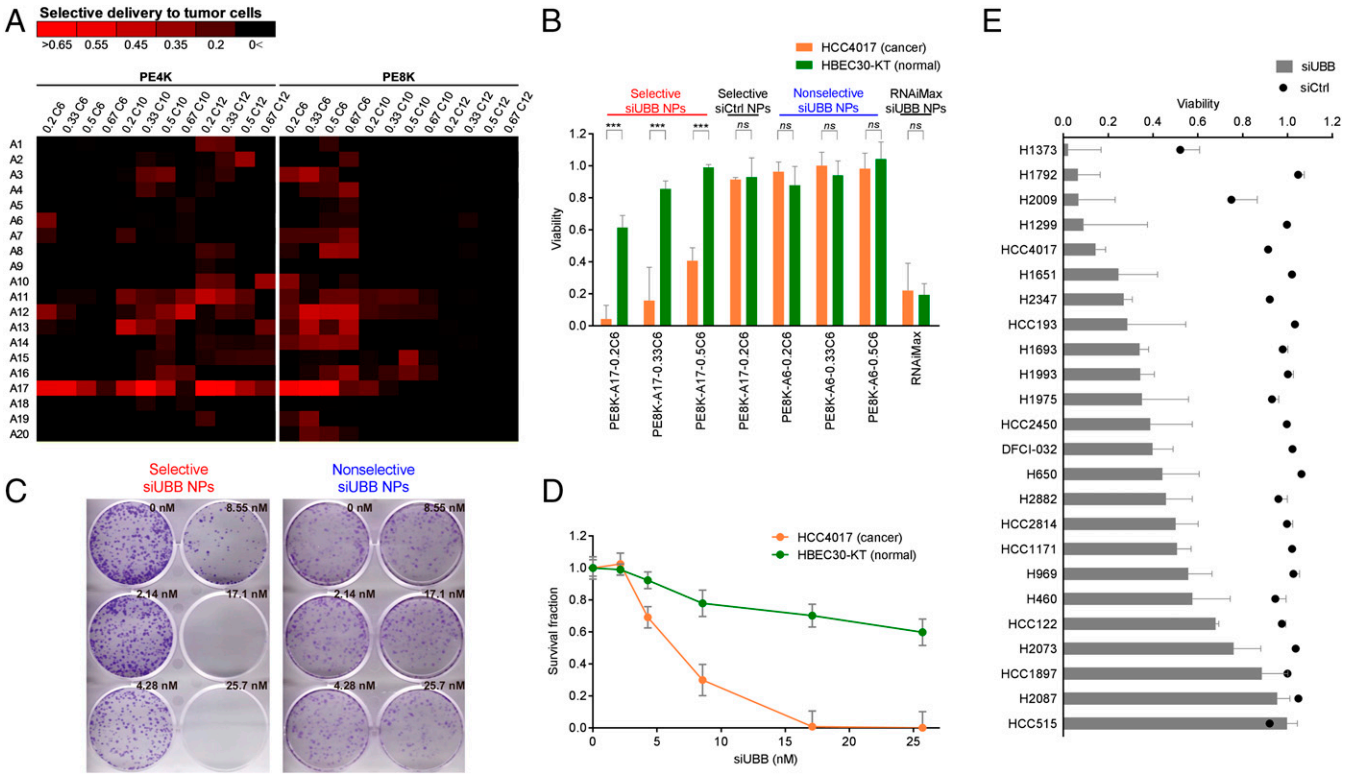


**Fig. 2.** Delivery of siUBB in functional polyester NPs was evaluated in patient-derived NSCLC lines to establish selectivity. (*A*) Polymer-siUBB NPs exhibited differential delivery efficacy to HCC4017 and HBEC30-KT cells. NPs were prepared at a weight ratio of 30:1 (polymer:siUBB) in citrate buffer (10 mM, pH 4.2). Cells were treated with siUBB NPs (34.2 nM siUBB) for 6 h followed by a 3-d incubation. Cell viability was quantified to compare treatments. Data are expressed as fold-increase in delivery selectivity toward cancer cells over normal cells. The full data set for each cell line appears in *SI Appendix*, Table S1. (*B*) Activity was validated and compared with a commercial control reagent (RNAiMax). Cancer-selective polymers (modification with A17 and C6SH) and control nonselective polymers (modified with A6 and C6SH) show consistent batch-to-batch delivery activity and selectivity in validation repeat assays (mean ± SD, $n = 3$). Statistical significance was determined using a two-tailed Student's *t* test (***, $P \leq 0.001$; *ns*, $P > 0.05$). (*C*) Selective siUBB NPs (PE8K-A17-0.2C6 siUBB polyplex NPs) inhibited the colony formation of HCC4017 cells (*Left*), whereas nonselective siUBB NPs (PE8K-A6-0.2C6 siUBB polyplex NPs) did not (*Right*). (*D*) Survival fraction curves show that the colony formation of HCC4017 tumor cells is completely inhibited by selective siUBB NPs at 17.1 nM, whereas >75% of normal HBEC30-KT cells survive when treated with this dose (mean ± SD, $n = 3$). (*E*) Selective siUBB NPs were able to kill the majority of an increased panel of patient-derived NSCLC cell lines (mean ± SD, $n = 3$).

**Lung Cancer-Selective Polyplex NPs Were Discovered Through Utilization of a Single Patient-Derived Cancer/Normal Cell Line Pair.** To investigate the potential of functional polyesters to be cancer specific, we delivered a pan-toxic siRNA targeting *UBB* (27, 28) to lung cancer and normal cells derived from single patient to discover cancer cell-selective NPs that show more efficacious siUBB delivery to tumor cells over matched normal cells (Fig. 2*A* and *SI Appendix*, Table S1). Treatment with free siUBB or NPs containing control siRNA (siCtrl) showed >90% cell viability for both cell lines under these delivery conditions. A number of functional polyester NPs enabled effective siUBB delivery to both cancer and normal cells (*SI Appendix*, Table S1). To identify the polyplexes that promoted siRNA delivery to cancer cells over normal cells, the difference in the decrease of cell viability (HBEC30-KT viability – HCC4017 viability) was plotted (Fig. 2*A*). This allowed identification of >100 cancer-selective polymers. Notably, A17-0.2C6 modified polymers enabled a 14-fold preferential cell killing to tumor cells. To verify that delivery activity and selectivity was reproducible, we resynthesized all key polymers in larger scale and compared them directly to a well-known transfection reagent (Fig. 2*B*). We found that functional polyester-mediated selectivity was consistent. In contrast, RNAiMax showed nearly identical delivery to both tumor and normal cells (80% cell death in both lines at 34.2 nM siUBB). As additional controls, PE8K-A17-0.2C6 siCtrl and PE8K-A6 siUBB NPs did not cause appreciable death in either cell line.

We next examined whether PE8K-A17-0.2C6 siUBB polyplex NPs (hereafter denoted as "selective siUBB NPs") (*SI Appendix*, Fig. S6) could inhibit growth of tumor colonies by conducting a colony formation assay (Fig. 2*C*). Selective siUBB NPs could completely abolish colony formation at doses as low as 17.1 nM siUBB. As a control, PE8K-A6-0.2C6 siUBB polyplex NPs (denoted as "nonselective siUBB NPs") show >75% survival fraction at the same dose. Interestingly, these two series of NPs possess nearly identical size, surface charge, and siUBB binding (*SI Appendix*, Fig. S7), but different delivery capability to tumor cells (Fig. 2 *A*–*C*). Particular side-chain functionalities may regulate endocytosis and control siRNA intracellular release. The selectivity of selective siUBB NPs to colony formation of cancer versus normal cells is compared in Fig. 2*D*. The survival fraction of HBEC30-KT (by cell counting) was more than 70% after treatment with 17.1 nM selective siUBB NPs, whereas no HCC4017 tumor clones formed at this dose (see consistency of cell and clone counting in *SI Appendix*, Fig. S8).

To further examine the efficacy of selective siUBB NPs, we extended the screen to a panel of 24 non–small-cell lung cancer (NSCLC) cell lines derived from The University of Texas Southwestern Medical Center (UTSW) patients over the years (Fig. 2*E*). Selective siUBB NPs can transfect most of the HCC NSCLC cell lines from our clinic, but not all lines are equally sensitive. We found that even cognate cells respond differently to the same polymer NP, implying that cellular differences should be carefully considered when evaluating any NP-mediated gene therapy. Moreover, we examined an additional 15 cell lines, representative of prostate, breast, liver, colorectal, head and neck, melanoma, ovarian, and pancreatic cancer. Similar to the NSCLC results, selective NPs were effective in most lines and displayed a unique differential delivery capability (*SI Appendix*, Fig. S9). To understand this effect further, we investigated the mechanism of selectivity and evaluated the ability of selective NPs to preferentially deliver siRNA to cancer cells in vitro and in vivo.

**Differential Cellular Uptake and Intracellular Dynamics Contributed to Selective Delivery to Cancer over Normal Cells.** One key to this study was that combinatorial modification of polyesters with various functional thiols provided the opportunity to diversify the physicochemical properties to overcome a series of delivery barriers. This has been shown to be difficult to realize through rational design of a single polymer (7, 8, 45). Overall, 137 polymers (29% of the library) exhibited preferential delivery to cancer cells (Fig. 2*A*). However, a large number of polymers also exhibited strong delivery to normal cells (*SI Appendix*, Table S1). Among the 137 selective polymers, the emergence of cysteamine (A17) suggests that this functional group may promote internalization through specialized pathways that reduce trafficking to lysosomes, thereby enhancing siRNA release inside of cancer cells (33, 42, 46–51). Previous reports on cysteamine-functionalized dendrimers (48) and the cell-penetrating peptide Pep-1 (49–51) that contain terminal cysteamine groups suggest that membrane binding and uptake is dependent on this functional group. Overall, the physical properties of the polymers clearly play a role in defining intracellular uptake and siRNA delivery efficacy, as polyplexes with high binding, small size, and positive surface charge were the most likely to be efficacious (*SI Appendix*, Fig. S10). However, the data also show that selectivity toward different cells is dependent on the chemistry of the NPs and not on the size, binding, or charge (*SI Appendix*, Fig. S7). We therefore speculate that cysteamine, or the resulting physical properties provided by this modification, could play an active role in cell membrane binding, and subsequent endocytosis due to differences in protein or lipid expression on cell surfaces.

To investigate the delivery mechanism, we tracked cellular uptake of selective NPs containing Cy5.5-labeled siRNA to cancer and normal cell lines using confocal microscopy (Fig. 3). After 30 min, selective NPs were observed on the cell membrane of both cell lines, visualized by a ring-like Cy5.5-siRNA signal on the cell surface. After 1 h, the fate differentiated between the two cell lines. Within this initial hour, selective Cy5.5-siRNA NPs internalized into HCC4017 cancer cells. In contrast, selective NPs were arrested on the cell membrane of HBEC30-KT normal cells throughout the duration of the incubation time (6 h) (Fig. 3*A*). Cellular uptake studies with various endocytosis inhibitors show that internalization of selective NPs to HCC4017 is dominated by the clathrin-dependent pathway (Fig. 3*B*). With longer incubation time (24–72 h), some selective NPs are internalized into HBEC30-KT and they completely colocalize with lysosomes (Fig. 3*C* and *SI Appendix*, Fig. S11). In contrast, a large amount of siRNA remains outside of lysosomes up to 72 h in HCC4017 cells. The presence of this free siRNA may explain why the silencing of targeted mRNA in the cytoplasm is more effective in HCC4017. Plotting of siRNA (red) versus lysosomes (green) illustrates this differential behavior, confirmed by calculation of Pearson's coefficient ($r_p$) (52) (Fig. 3*C*). Overall, these data clearly show that the two cell lines respond differently to the same NP.

As a further investigation of intracellular dynamics, we measured possible exocytosis of siRNA because reports have shown that free siRNA in the cytoplasm delivered by lipid NPs can be exocytosed from cells (53). By measuring extracellular fluorescence after administration of Cy5.5-labeled siRNA in NPs, results indicated that only a very limited (<4%) amount of siRNA was exocytosed from both cell lines up to 72 h (*SI Appendix*, Fig. S12). There was no statistical difference in the amount of exocytosed siRNA between the two cell lines. In addition, we studied the release of siRNA from NPs using an siRNA fluorescence resonance energy transfer (FRET) pair (siAF594/siAF647) (54) (*SI Appendix*, Fig. S13). When examining FRET, more RNA was measured inside of HCC4017 cells compared with HBEC30-KT, indicating greater NP disassembly. These FRET experiments, combined with the difference in lysosome colocalization (Fig. 3*B*), indicate that HCC4017 endocytoses selective NPs faster and to a greater extent than normal cells, and also promotes enhanced siRNA release. Together, these experiments reveal differential cellular responses to the same NP that account for the improved cancer cell efficacy.

**Cancer-Selective NPs Enabled Extended Retention in Xenograft Tumors.** We next examined the capability of selective NPs to preferentially internalize and be retained in tumors in vivo. s.c. HCC4017 tumor xenografts were formed in nude mice and injected with free

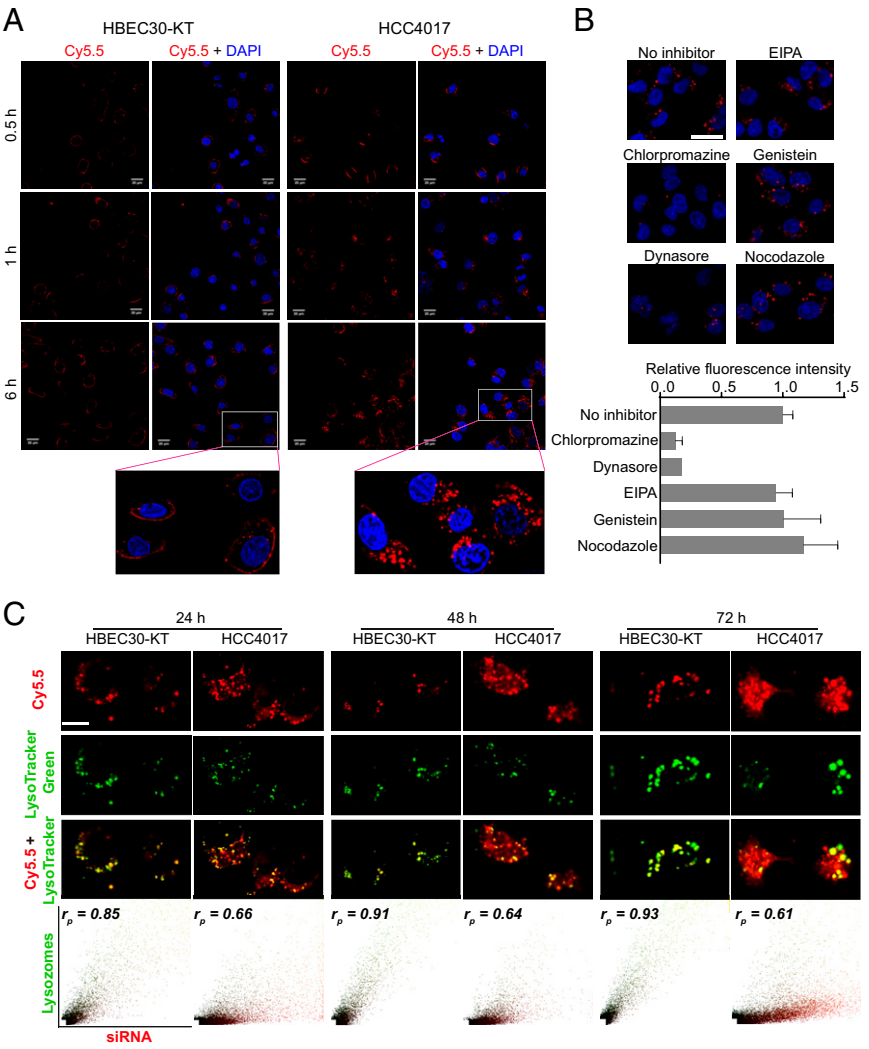


**Fig. 3.** Selective Cy5.5 NPs preferentially internalized into HCC4017 cancer cells. (*A*) Selective Cy5.5 NPs (PE8K-A17-0.2C6 Cy5.5-siRNA polyplex NPs) were effectively endocytosed into HCC4017 cancer cells within 1 h. In contrast, the identical NPs remain arrested at the cell membrane of HBEC30-KT normal cells even after 6 h. A single batch of NPs was applied in parallel to the two cell lines (34.2 nM Cy5.5-siRNA, same dose as in Fig. 2 siUBB delivery experiments). After 0.5-, 1-, or 6-h treatment with NPs, cells were washed with PBS, fixed with paraformaldehyde [4% (vol/vol)], and stained with DAPI for confocal microscopy. (Scale bar, 20 μm.) (*Inset*) A higher-magnification inset clearly shows selective Cy5.5 NPs along the membrane of HBEC30-KT normal cells and internalized as defined puncta in HCC4017 cancer cells. Further incubation (24–72 h, *SI Appendix*, Fig. S11) in growth media leads to limited internalization of NPs into HBEC30-KT normal cells. (*B*) Cellular uptake with endocytosis inhibitors shows that the internalization of selective Cy5.5 NPs to HCC4017 is dominated by clathrin-dependent endocytosis. (Scale bar, 30 μm.) (*C*) The colocalization with LysoTracker green indicates that Cy5.5-siRNA is completely trapped within lysosomes in the normal cells whereas a large fraction of siRNA remains out of lysosomes in HCC4017 cancer cells. This results in selective killing between tumor and normal cells. (*Bottom*) A plot of siRNA (red) versus lysosomes (green) illustrates colocalization. Pearson's coefficient ($r_p$) is expressed. (Scale bar, 20 μm.)

Cy5.5-siRNA, nonselective Cy5.5-siRNA NPs, or selective Cy5.5-siRNA NPs. Fluorescence tracking was used to measure the decay kinetics of Cy5.5-siRNA from the tumor. Selective NPs provided extended retention of Cy5.5-siRNA (Fig. 4) inside of the tumors, which then resulted in increased efficacy (Fig. 5).

Selective NPs stayed inside of the tumors for more than 1 wk, whereas nonselective NPs were cleared after about 6 h. Free Cy5.5-siRNA also quickly diffused away from the tumor (Fig. 4*A*). Using the same imaging settings, only the selective Cy5.5-siRNA NPs showed fluorescence after 24 h. Moreover, Cy5.5-siRNA was retained in the tumor for more than 6 d. The decay of the normalized fluorescence intensity ($I_t/I_0$) in these tumors quantified the retention effect of selective NPs due to degradation and diffusion of Cy5.5-siRNA in tumor tissues (Fig. 4*C*). To verify the time- and polyplex-dependent Cy5.5-siRNA retention, we harvested tumors and imaged tumor sections. Fluorescence imaging verified the retention observed in whole animal imaging (Fig. 4*B*). To examine the effect of the polymer itself, we synthesized a Cy5.5-labeled selective polymer (PE8K-A17-0.2C6-Cy5.5). When injected into HCC4017 xenograft tumors, Cy5.5-labeled polymer NPs (no siRNA) were also retained in the tumors for >5 d (*SI Appendix*, Fig. S14). We next encapsulated Doxorubicin (Dox) into the selective NPs to examine a model chemotherapeutic drug-loaded NP, and performed similar retention studies. Again, the Dox-loaded NPs were retained for >5 d. These results clearly show that the physical chemistry of the NP provides the retention effect. The retention behavior is therefore not limited to siRNA polyplexes, which may provide future opportunities to selectively deliver other anticancer drugs.

**Cancer-Selective Polyplex NPs Significantly Suppressed Tumor Growth by Enhancing siUBB-Mediated Apoptosis.** To further examine the anticancer effects of selective NPs, we performed a long-term HCC4017

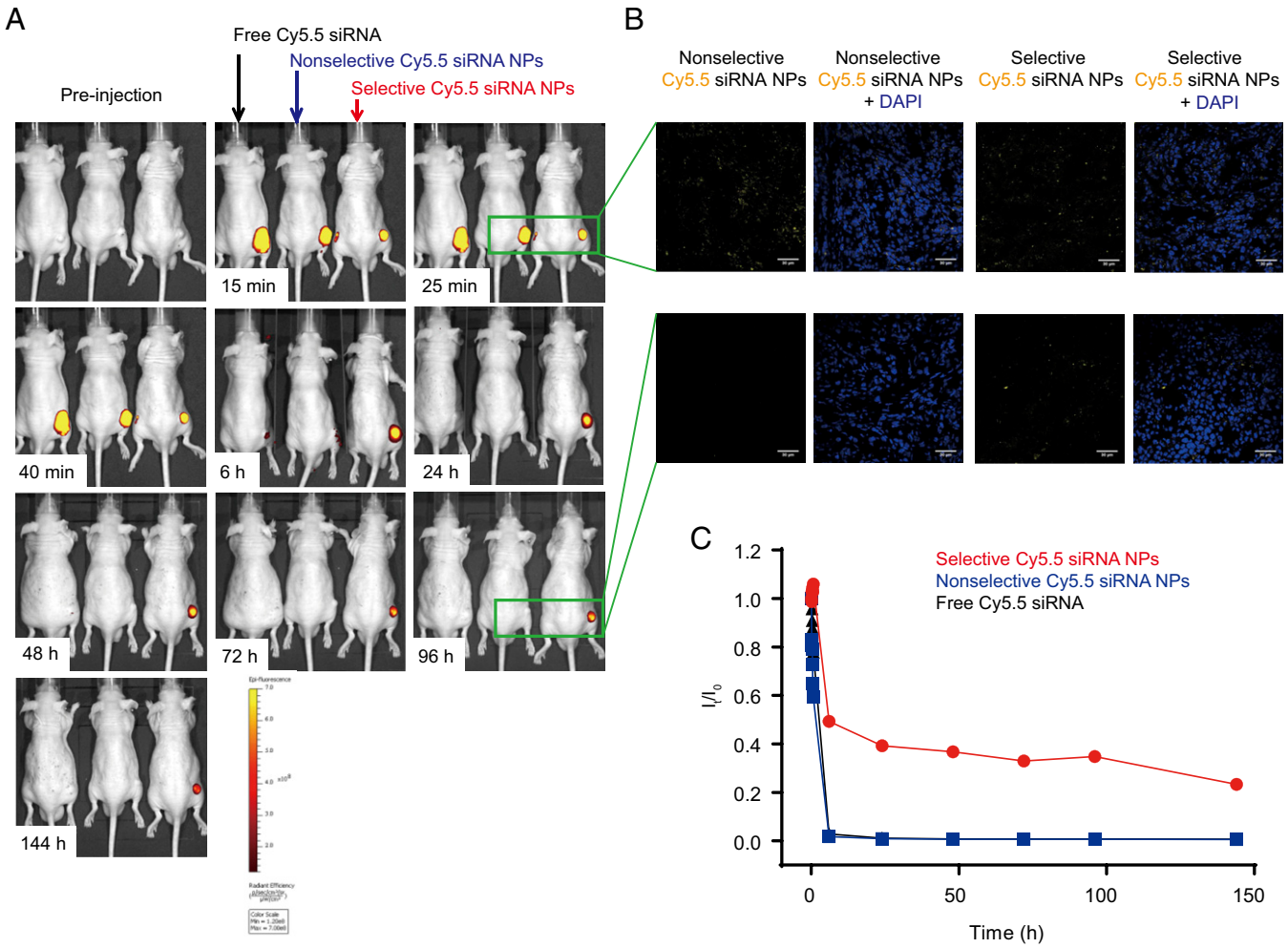


**Fig. 4.** Cancer-selective siRNA NPs provide extended retention inside of tumor tissues. (*A*) Fluorescence imaging of live mice after intratumoral injection with free Cy5.5-siRNA, selective Cy5.5 NPs, or nonselective Cy5.5 NPs. NPs (polymer/siRNA, 30/1, wt/wt) were prepared by mixing polymer DMSO solution into Cy5.5-siRNA citrate buffer (10 mM, pH 4.2) followed by dialysis (cutoff MW of 3,500) against PBS for 1 h; 30 μL of NPs or free Cy5.5-siRNA (2.4 μg) were injected into the tumor. The intratumoral injections were performed in triplicate and representative images of mice appear at different time points (0–144 h). (*B*) Representative confocal microscopy images of 8-μm-thick tumor tissue slices taken from mice at 25 min (*Top*) and 96 h (*Bottom*) postinjection confirm the presence and absence of siRNA. (Scale bar, 30 μm.) (*C*) Fluorescence decay ($I_t/I_0$) was obtained by normalizing the intensity ($I_t$) to that at 15 min ($I_0$). A plot of intensity versus time shows that selective Cy5.5 NPs enable sustained retention of siRNA in tumor tissue (mean ± SD, $n = 3$).

tumor growth inhibition experiment. Once all tumors reached a size of 110 $mm^3$, we injected PBS, nonselective siUBB NPs, selective siCtrl NPs, or selective siUBB NPs. Mice received intratumoral injections of 0.12 mg/kg siUBB on days 20, 25, and 30 (Fig. 5*A*). Tumor volume measurements show that selective siUBB NPs significantly suppressed the growth of xenograft tumors (Fig. 5 *A* and *B*). The absence of any weight loss indicated no appreciable toxicity. Even though the nonselective NPs caused some cell death (Fig. 5 *C* and *D*), only the selective NPs affected tumor growth. The prolonged retention of selective NPs in tumors (Fig. 4), combined with enhancement of delivery to tumor cells (Fig. 2 *A* and *B*), resulted in significant growth suppression (Fig. 5 *A* and *B*).

To verify successful delivery, we analyzed siUBB-mediated apoptosis of tumor cells. Silencing of *UBB* causes apoptosis through multiple pathways, including interactions with Fas-like inhibitor protein, the proapoptotic Bcl-2 family member BAX, and TRAIL signaling (27). First, we measured caspase-3/7 activity 4-d postinjection as an indicator of programmed cell death. Quantitative caspase activity in tumor tissues show that nonselective siUBB NPs cause ~2-fold increase in apoptosis, whereas selective siUBB NPs cause >12-fold increase in tumor cell apoptosis (Fig. 5*C*). Next, we performed TUNEL assays on histological slides to visualize DNA fragmentation. Without injection, TUNEL staining shows minimal apoptosis. The apoptosis signal increased only slightly when siUBB was encapsulated in nonselective NPs. After injection of selective siUBB NPs, the area and density of the green fluorescence increased dramatically, showing that the activity of encapsulated siUBB is enhanced by the cancer-selective NPs. Accordingly, much more necrosis (shown as fewer nuclei in blue) was observed by H&E staining (Fig. 5*D*), explaining why siUBB delivery inside of selective NPs arrested the growth of xenograft tumors.

**Cancer-Selective NPs Enabled Gene Silencing in Xenograft and Orthotopic Lung Tumors.** To more broadly examine the utility of selective NPs, we expanded the type of tumor model, NSCLC cells, and administration methods. The ability to deliver NPs i.v. and through aerosolized spray is critically important for ultimate lung cancer translation. Because siUBB can have off-target toxicity in circulating cells, we examined i.v. delivery of siLuc to luciferase reporter expressing tumors. We created HCC2814-Luc xenografts and measured targeted siRNA silencing in tumors after i.v. administration of siLuc NPs. The luciferase signal in the tumor slightly increased in 24–48 h for the mice that were injected with 1 mg/kg

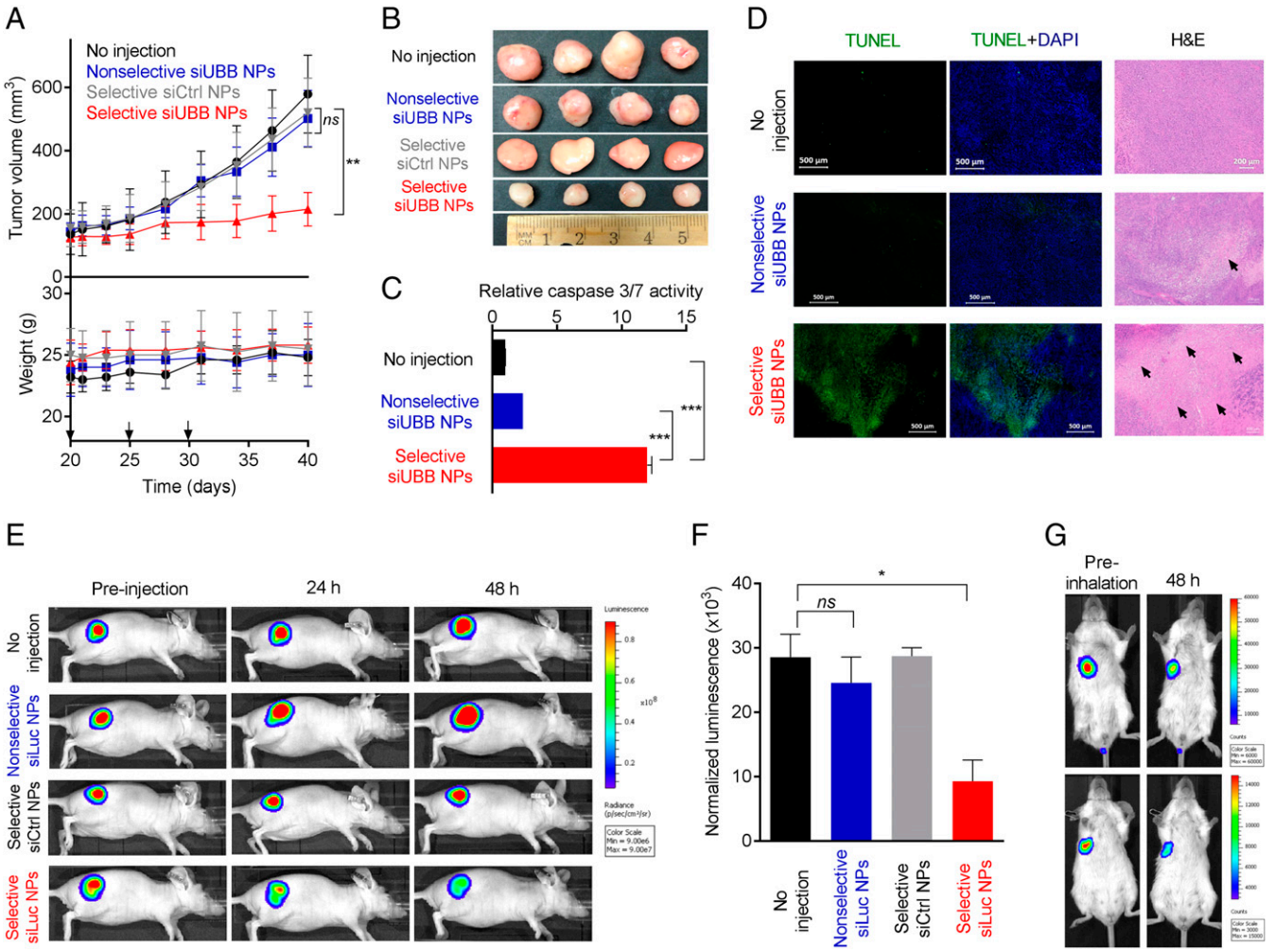


**Fig. 5.** Cancer-selective NPs enhance siRNA-mediated gene silencing in vivo. (*A*) Selective and nonselective siUBB NPs were injected into HCC4017 xenograft tumors to compare selective delivery potential in vivo. Time course of tumor volume and mouse weight (mean ± SD, $n = 4$). The arrows indicate the administration of siUBB NPs at days 20, 25, and 30. (*B*) Photographs of the excised tumors at the end of the study (20-d post-first NP injection; 40-d post-tumor cell implantation). (*C*) Injection of selective siUBB NPs induced fivefold higher caspase-3/7 activity compared with controls, demonstrating greater apoptosis and potent delivery of siUBB by the cancer-selective NPs (mean ± SD, $n = 3$). Arrows indicate regions of necrosis. (*D*) After 4 d, the tumors were harvested. A TUNEL assay was performed on representative 8-μm-thick, paraffin-embedded tumor tissue slices. Fluorescence images indicate that the sustained retention of cancer-selective siUBB polyplexes results in greater apoptosis. (Scale bar, 500 μm.) H&E images show greater necrosis in tumors that received cancer-selective siUBB NPs. (Scale bar, 200 μm.) (*E*) i.v. injection of selective siLuc NPs induces luciferase knockdown in HCC2814-Luc xenograft tumors (1 mg/kg siLuc) in 48 h. One of four mice was shown as a representative for each group. (*F*) Efficient luciferase knockdown was confirmed by the decrease of protein content normalized luminance in the homogenized HCC2814-Luc tumor tissue with injection of selective siLuc NPs (mean ± SD, $n = 4$). (*G*) Selective siLuc NPs enable significant luciferase knockdown in HCC1299-Luc orthotopic lung tumors after administrated through aerosol inhalation. Statistical significance was determined using a two-tailed Student's *t* test (***, $P \leq 0.001$; **, $P \leq 0.01$; *, $P \leq 0.05$; *ns*, $P > 0.05$).

nonselective siLuc NPs, selective siCtrl NPs, or PBS because there was no sufficient suppression of the luciferase expression in the cancer cells. After i.v. administration of 1 mg/kg selective siLuc NPs, the luciferase signal decreased due to successful luciferase silencing in the tumor tissue (Fig. 5*E*). Harvested tumors were homogenized to quantify luciferase expression on a total protein normalized level. Results indicated that i.v. injection of the selective siLuc NPs led to ~70% luciferase knockdown in xenograft tumors (Fig. 5*F*).

Finally, to further extend the translational impact of this selective NP system, we evaluated silencing ability of aerosolized NPs to an orthotopic lung cancer model. We chose a cell line (HCC1299) from our NSCLC screen that was known to colonize in the lung after i.v. administration and form orthotopic lung tumors. Selective siLuc NPs were aerosolized and delivered to mice harboring orthotopic HCC1299-Luc lung tumors. After aerosol inhalation of selective siLuc NPs, the luciferase signal in the lung tumors significantly decreased after 48 h (Fig. 5*G*). Aerosol inhalation of selective NPs may be the preferred approach in the clinic. Cumulatively, these results demonstrate selective uptake and retention in tumor cells in multiple in vivo models and cell lines. This approach therefore provides a promising way to improve cancer therapy by increasing cancer selectivity.

## Discussion

To minimize the side effects of conventional nontargeted chemo- and small-RNA therapeutics, we examined the hypothesis that the physiochemical properties of materials alone could endow selective delivery to specific cells. We discovered selective NPs that efficiently transfect HCC4017 lung cancer cells in vitro and in vivo, but not matched normal lung cells from the same patient. This approach has proved valuable for the discovery of small-molecule drugs and identification of genetic cancer vulnerabilities (55). We now show that it can be used to discover drug carriers that are specific to cancer cells. This work establishes feasibility of this approach to

increase on-target drug activity. It also illuminates the unappreciated reality that NP carriers exhibit cell type-dependent delivery.

In this paper, we have described an approach to enhance cancer cell delivery that does not require targeting ligand modification. This delivery carrier-based selectivity could potentially synergize with personalized medicine strategies to transform patient-centered decision making by providing customized drugs and delivery vehicles according to individual genetic profiles (56, 57). It also highlights that fundamental cellular differences have not been fully understood in the development of delivery carriers for cancer therapy, particularly for RNA-based therapeutics. Through selectivity screening on a cancer–normal cell pair and additional NSCLC cell lines, it is clear that cells respond differently to the same NP. Most papers focus on a single cell line from a single cancer type. We demonstrate that delivery efficacy and selectivity is highly cell line-dependent, which is an unexplored phenomenon in drug delivery. It is imagined that cell-type specificity of delivery carriers in vivo could alter the efficacy of clinical gene therapies and patient outcomes. This should be carefully considered in choosing molecular targets and developing targeted delivery carriers.

## Methods

Detailed materials, methods, and additional figures are provided in *SI Appendix*. This includes descriptions of chemical synthesis and characterization, preparation and characterization of NPs, in vitro and in vivo gene silencing, animal studies, and statistics. All experiments were approved by the Institutional Animal Care and Use Committees of The University of Texas Southwestern Medical Center and were consistent with local, state, and federal regulations as applicable.

**ACKNOWLEDGMENTS.** We thank Dr. Michael Peyton for providing helpful advice on culturing the cell lines. We also thank Professor Michael White and Ms. Elizabeth McMillan for providing helpful suggestions. D.J.S. gratefully acknowledges financial support from the Cancer Prevention and Research Institute of Texas (CPRIT) (Grant R1212), Welch Foundation (Grant I-1855), American Cancer Society (Grant ACS-IRG-02-196), UTSW Friends of the Comprehensive Cancer Center 2014 Award in Cancer Research, and UTSW Translational Pilot Program via the NIH (Grant UL1TR001105). J.B.M. was supported by a CPRIT Fellowship (Grant RP140110). J.D.M. acknowledges support from an NIH National Cancer Institute SPORE grant in Lung Cancer (P50CA70907) and CPRIT Grants RP110708 and RP120732. The content is solely the responsibility of the authors and does not necessarily represent the official views of any of the above mentioned funding agencies.

1. Siegel R, Ma J, Zou Z, Jemal A (2014) Cancer statistics, 2014. *CA Cancer J Clin* 64(1):9–29.
2. Moding EJ, Kastan MB, Kirsch DG (2013) Strategies for optimizing the response of cancer and normal tissues to radiation. *Nat Rev Drug Discov* 12(7):526–542.
3. Brannon-Peppas L, Blanchette JO (2004) Nanoparticle and targeted systems for cancer therapy. *Adv Drug Deliv Rev* 56(11):1649–1659.
4. Cheng CJ, Tietjen GT, Saucier-Sawyer JK, Saltzman WM (2015) A holistic approach to targeting disease with polymeric nanoparticles. *Nat Rev Drug Discov* 14(4):239–247.
5. Wu SY, Lopez-Berestein G, Calin GA, Sood AK (2014) RNAi therapies: Drugging the undruggable. *Sci Transl Med* 6(240):240ps7.
6. Collins I, Workman P (2006) New approaches to molecular cancer therapeutics. *Nat Chem Biol* 2(12):689–700.
7. Whitehead KA, Langer R, Anderson DG (2009) Knocking down barriers: Advances in siRNA delivery. *Nat Rev Drug Discov* 8(2):129–138.
8. Kanasty R, Dorkin JR, Vegas A, Anderson D (2013) Delivery materials for siRNA therapeutics. *Nat Mater* 12(11):967–977.
9. Jackson AL, Linsley PS (2010) Recognizing and avoiding siRNA off-target effects for target identification and therapeutic application. *Nat Rev Drug Discov* 9(1):57–67.
10. Whitehead KA, Dahlman JE, Langer RS, Anderson DG (2011) Silencing or stimulation? siRNA delivery and the immune system. *Annu Rev Chem Biomol Eng* 2:77–96.
11. Smith BR, et al. (2014) Selective uptake of single-walled carbon nanotubes by circulating monocytes for enhanced tumour delivery. *Nat Nanotechnol* 9(6):481–487.
12. Voigt J, Christensen J, Shastri VP (2014) Differential uptake of nanoparticles by endothelial cells through polyelectrolytes with affinity for caveolae. *Proc Natl Acad Sci USA* 111(8):2942–2947.
13. Song E, et al. (2005) Antibody mediated in vivo delivery of small interfering RNAs via cell-surface receptors. *Nat Biotechnol* 23(6):709–717.
14. McNamara JO, 2nd, et al. (2006) Cell type-specific delivery of siRNAs with aptamer-siRNA chimeras. *Nat Biotechnol* 24(8):1005–1015.
15. Davis ME, et al. (2010) Evidence of RNAi in humans from systemically administered siRNA via targeted nanoparticles. *Nature* 464(7291):1067–1070.
16. Ashley CE, et al. (2011) The targeted delivery of multicomponent cargos to cancer cells by nanoporous particle-supported lipid bilayers. *Nat Mater* 10(5):389–397.
17. Rozema DB, et al. (2007) Dynamic PolyConjugates for targeted in vivo delivery of siRNA to hepatocytes. *Proc Natl Acad Sci USA* 104(32):12982–12987.
18. Carven GJ, et al. (2004) Monoclonal antibodies specific for the empty conformation of HLA-DR1 reveal aspects of the conformational change associated with peptide binding. *J Biol Chem* 279(16):16561–16570.
19. Tenzer S, et al. (2013) Rapid formation of plasma protein corona critically affects nanoparticle pathophysiology. *Nat Nanotechnol* 8(10):772–781.
20. Anselmo AC, Mitragotri S (2014) An overview of clinical and commercial impact of drug delivery systems. *J Control Release* 190:15–28.
21. Pounder R, Dove A (2010) Towards poly(ester) nanoparticles: Recent advances in the synthesis of functional poly(ester)s by ring-opening polymerization. *Polym Chem* 1(3):260–271.
22. Yan Y, Siegwart DJ (2014) Scalable synthesis and derivation of functional polyesters bearing ene and epoxide side chains. *Polym Chem* 5(4):1362–1371.
23. Hao J, et al. (2015) Rapid synthesis of a lipocationic polyester library via ring-opening polymerization of functional valerolactones for efficacious siRNA delivery. *J Am Chem Soc* 137(29):9206–9209.
24. Tian HY, Tang ZH, Zhuang XL, Chen XS, Jing XB (2012) Biodegradable synthetic polymers: Preparation, functionalization and biomedical application. *Prog Polym Sci* 37(2):237–280.
25. Hoyle CE, Lowe AB, Bowman CN (2010) Thiol-click chemistry: A multifaceted toolbox for small molecule and polymer synthesis. *Chem Soc Rev* 39(4):1355–1387.
26. Ramirez RD, et al. (2004) Immortalization of human bronchial epithelial cells in the absence of viral oncoproteins. *Cancer Res* 64(24):9027–9034.
27. Zhang HG, Wang J, Yang X, Hsu HC, Mountz JD (2004) Regulation of apoptosis proteins in cancer cells by ubiquitin. *Oncogene* 23(11):2009–2015.
28. Wu P, et al. (2010) Ubiquitin B: An essential mediator of trichostatin A-induced tumor-selective killing in human cancer cells. *Cell Death Differ* 17(1):109–118.
29. Kurisawa M, Yokoyama M, Okano T (2000) Transfection efficiency increases by incorporating hydrophobic monomer units into polymeric gene carriers. *J Control Release* 68(1):1–8.
30. Akinc A, et al. (2008) A combinatorial library of lipid-like materials for delivery of RNAi therapeutics. *Nat Biotechnol* 26(5):561–569.
31. Love KT, et al. (2010) Lipid-like materials for low-dose, in vivo gene silencing. *Proc Natl Acad Sci USA* 107(5):1864–1869.
32. Semple SC, et al. (2010) Rational design of cationic lipids for siRNA delivery. *Nat Biotechnol* 28(2):172–176.
33. Siegwart DJ, et al. (2011) Combinatorial synthesis of chemically diverse core-shell nanoparticles for intracellular delivery. *Proc Natl Acad Sci USA* 108(32):12996–13001.
34. Jayaraman M, et al. (2012) Maximizing the potency of siRNA lipid nanoparticles for hepatic gene silencing in vivo. *Angew Chem Int Ed Engl* 51(34):8529–8533.
35. Nelson CE, et al. (2013) Balancing cationic and hydrophobic content of PEGylated siRNA polyplexes enhances endosome escape, stability, blood circulation time, and bioactivity in vivo. *ACS Nano* 7(10):8870–8880.
36. Alabi CA, et al. (2013) Multiparametric approach for the evaluation of lipid nanoparticles for siRNA delivery. *Proc Natl Acad Sci USA* 110(32):12881–12886.
37. Dong Y, et al. (2014) Lipopeptide nanoparticles for potent and selective siRNA delivery in rodents and nonhuman primates. *Proc Natl Acad Sci USA* 111(11):3955–3960.
38. Whitehead KA, et al. (2014) Degradable lipid nanoparticles with predictable in vivo siRNA delivery activity. *Nat Commun* 5:4277.
39. deRonde BM, et al. (2016) Optimal hydrophobicity in ring-opening metathesis polymerization-based protein mimics required for siRNA internalization. *Biomacromolecules* 17(6):1969–1977.
40. Eltoukhy AA, et al. (2012) Effect of molecular weight of amine end-modified poly (β-amino ester)s on gene delivery efficiency and toxicity. *Biomaterials* 33(13):3594–3603.
41. Mok H, Lee SH, Park JW, Park TG (2010) Multimeric small interfering ribonucleic acid for highly efficient sequence-specific gene silencing. *Nat Mater* 9(3):272–278.
42. Tzeng SY, Hung BP, Grayson WL, Green JJ (2012) Cystamine-terminated poly(beta-amino ester)s for siRNA delivery to human mesenchymal stem cells and enhancement of osteogenic differentiation. *Biomaterials* 33(32):8142–8151.
43. Scholz C, Wagner E (2012) Therapeutic plasmid DNA versus siRNA delivery: Common and different tasks for synthetic carriers. *J Control Release* 161(2):554–565.
44. Zhou K, et al. (2016) Modular degradable dendrimers enable small RNAs to extend survival in an aggressive liver cancer model. *Proc Natl Acad Sci USA* 113(3):520–525.
45. Sahay G, Alakhova DY, Kabanov AV (2010) Endocytosis of nanomedicines. *J Control Release* 145(3):182–195.
46. Tzeng SY, Green JJ (2013) Subtle changes to polymer structure and degradation mechanism enable highly effective nanoparticles for siRNA and DNA delivery to human brain cancer. *Adv Healthc Mater* 2(3):468–480.
47. Kozielski KL, Tzeng SY, De Mendoza BAH, Green JJ (2014) Bioreducible cationic polymer-based nanoparticles for efficient and environmentally triggered cytoplasmic siRNA delivery to primary human brain cancer cells. *ACS Nano* 8(4):3232–3241.
48. Amir RJ, et al. (2011) Multifunctional trackable dendritic scaffolds and delivery agents. *Angew Chem Int Ed Engl* 50(15):3425–3429.
49. Henriques ST, Castanho MARB (2004) Consequences of nonlytic membrane perturbation to the translocation of the cell penetrating peptide pep-1 in lipidic vesicles. *Biochemistry* 43(30):9716–9724.
50. Henriques ST, Castanho MARB (2008) Translocation or membrane disintegration? Implication of peptide-membrane interactions in pep-1 activity. *J Pept Sci* 14(4):482–487.

51. Henriques ST, Castanho MARB, Pattenden LK, Aguilar MI (2010) Fast membrane association is a crucial factor in the peptide pep-1 translocation mechanism: A kinetic study followed by surface plasmon resonance. *Biopolymers* 94(3):314–322.
52. French AP, Mills S, Swarup R, Bennett MJ, Pridmore TP (2008) Colocalization of fluorescent markers in confocal microscope images of plant cells. *Nat Protoc* 3(4): 619–628.
53. Sahay G, et al. (2013) Efficiency of siRNA delivery by lipid nanoparticles is limited by endocytic recycling. *Nat Biotechnol* 31(7):653–658.
54. Alabi CA, et al. (2012) FRET-labeled siRNA probes for tracking assembly and disassembly of siRNA nanocomplexes. *ACS Nano* 6(7):6133–6141.
55. Whitehurst AW, et al. (2007) Synthetic lethal screen identification of chemosensitizer loci in cancer cells. *Nature* 446(7137):815–819.
56. Xie Y, Minna JD (2008) Predicting the future for people with lung cancer. *Nat Med* 14(8):812–813.
57. Hamburg MA, Collins FS (2010) The path to personalized medicine. *N Engl J Med* 363(4):301–304.